

## Cyclohexene Adsorption and Reactions on Clean and Bismuth-Covered Pt(111)

JOSÉ A. RODRIGUEZ AND CHARLES T. CAMPBELL<sup>1</sup>

*Chemistry Department, Indiana University, Bloomington, Indiana 47405*

Received July 1, 1988; revised September 28, 1988

The chemisorption and dehydrogenation of cyclohexene on clean and bismuth-covered Pt(111) was studied using thermal desorption mass spectrometry (TDS), X-ray photoelectron spectroscopy (XRS), and Auger electron spectroscopy. Four different molecular cyclohexene desorption states appear in the thermal desorption spectra of cyclohexene on clean Pt(111). The temperatures and activation energies for desorption of these states are 158 K (9.1 kcal/mole), 190 K (11.0 kcal/mole), 255 K (15.0 kcal/mole), and 300 K (17.9 kcal/mole). The XPS data indicate that about 4.5 Pt(111) surface atoms are required on average to accommodate each adsorbed cyclohexene molecule. At low coverages ( $\Theta_{\text{C}_6\text{H}_{10}} < 0.05$  molecule per Pt atom) all the adsorbed cyclohexene dehydrogenates upon heating to produce adsorbed benzene (at temperatures below 350 K), which further decomposes on the surface by 800 K to give graphitic carbon and  $\text{H}_2$ . At high coverages of either cyclohexene or coadsorbed bismuth, the adsorbed cyclohexene and the product benzene molecularly desorb from the surface. A different intermediate in cyclohexene dehydrogenation is stabilized at these high coverages (perhaps  $\pi$ -allyl *c*- $\text{C}_6\text{H}_{9,a}$ ). During the TDS experiments on clean or Bi-dosed Pt(111), neither cyclohexadiene nor products of C-C bond breaking were detected with the mass spectrometer. The blocking of Pt surface sites with coadsorbed Bi adatoms, which have only minor electronic influences on the Pt sites, showed that the rate constants for diffusion and dehydrogenation of cyclohexene on Pt(111) are considerably larger than that for desorption. As a consequence, the effective ensemble requirement for cyclohexene dehydrogenation is relatively small, especially compared to benzene and cyclohexane. © 1989 Academic Press, Inc.

### I. INTRODUCTION

The importance of the dehydrogenation of cyclohexene ( $\text{C}_6\text{H}_{10}$  for abbreviation here) to produce benzene on Pt catalysts has given rise to a number of studies of the interactions of  $\text{C}_6\text{H}_{10}$  with Pt surfaces (1, 2, and references therein). The adsorption and reactions of  $\text{C}_6\text{H}_{10}$  on Pt(111) have been previously studied using thermal desorption mass spectrometry (TDS) (3), low-energy electron diffraction (LEED) (4), and work function measurements (4). Somorjai and co-workers (1, 4-6) investigated the catalytic activity of a Pt(111) surface for the dehydrogenation of cyclohexene to produce benzene under very low pressure conditions ( $\sim 10^{-6}$  Torr of  $\text{C}_6\text{H}_{10}$  and  $\text{H}_2$ ).

One objective of the present work is a detailed study of the adsorption and chemistry of  $\text{C}_6\text{H}_{10}$  on Pt(111). First, we investigate the different adsorption states of  $\text{C}_6\text{H}_{10}$  on Pt(111) and the mechanism of dehydrogenation of the adsorbed molecule using thermal desorption mass spectrometry and X-ray photoelectron spectroscopy. We then explore the ensemble (site-size) requirement for the dehydrogenation of adsorbed cyclohexene by following the kinetics of this reaction on the Pt(111) surface with controlled coverages of bismuth adatoms. The motivation for employing bismuth to probe site-size or ensemble requirements for surface reactions has been presented in detail in previous publications (7, 16) and is related to the fact that Bi adatoms are relatively inert in surface chemistry, spread uniformly over the surface, and

<sup>1</sup> Alfred P. Sloan Research Fellow.

have only a small amount of charge transfer with the Pt substrate. This present paper is part of a series of studies (7, 9–12) of the coadsorption of cyclic hydrocarbons (benzene, cyclohexane, cyclopentene, and cyclopentane) with Bi on Pt(111) where Bi has been utilized to investigate the ensemble requirements for surface reactions. Finally, we use a new method, bismuth postdosing in thermal desorption mass spectroscopy (BPTDS) (8), to investigate the molecular adsorbates produced from cyclohexene, showing that adsorbed benzene is the initial product of the dehydrogenation of cyclohexene on Pt(111).

## II. EXPERIMENTAL

The chemisorption and dehydrogenation of  $C_6H_{10}$  on clean and bismuth-covered Pt(111) surfaces were studied employing TDS, Auger electron spectroscopy (AES), and X-ray photoelectron spectroscopy (XPS). The characteristics of the ultrahigh vacuum apparatus (together with its sample manipulator and Bi doser) and the procedure employed for the preparation and cleaning of the Pt(111) crystal were described in a previous paper (9). All XPS spectra were collected with a Mg X-ray source. The spectrometer energy was calibrated using XPS and XAES transitions for pure Ag (26). Our XPS binding energy scale was referenced to the Pt( $4f_{7/2}$ ) peak for clean Pt(111), which we set at  $70.9 \pm 0.04$  eV binding energy (26). At the pass energy (100 eV) which we used for the XPS spectra reported here, the narrowest peaks showed a full width at half-maximum (FWHM) of  $1.65 \pm 0.05$  eV, which we take as the overall instrumental resolution. A linear background between the limits of a fixed window was subtracted from the XPS peaks in determining the areas of integrated XPS intensities reported here. The approximate window values used for the C( $1s$ ), Pt( $4f$ ), and Bi( $4f$ ) peaks were 287.5–279.75, 78.5–67.5, and 165.5–154.5 eV binding energy (B.E.), respectively. These Pt and Bi windows cover both the  $4f_{5/2}$  and the  $4f_{7/2}$

peaks. All XPS and AES spectra were collected with detection normal to the surface.

The cyclohexene employed in the experiments was from Aldrich, stated to be of greater than 99% purity. For dosing  $C_6H_{10}$ , we generally used a cosine-emitting pinhole doser such as that described previously (9). This was located  $\sim 8$  cm from the sample and gave an enhancement factor of  $\sim 2.5$  compared to dosing only from the background pressure. This enhancement factor was taken into consideration in reporting the exposures here. Cyclohexene was usually dosed onto the surfaces at a sample temperature of  $\sim 100$  K. In calculating exposures here, we used the ion gauge reading directly, without correction for the sensitivity factor for cyclohexene relative to  $N_2$ . However, in calculating the sticking coefficient, we used the reported relative ion gauge sensitivity factor of 6.4 for cyclohexene (13).

The TDS experiments were performed with a line-of-sight quadrupole mass spectrometer, using a feedback circuit in which the heating rate was held constant at  $0.286$  mV  $s^{-1}$  on the Chromel–Alumel thermocouple. This leads to a temperature rate of 11 to 7 K  $s^{-1}$  between 120 and 250 K and to a constant value of 7 K  $s^{-1}$  above 250 K. The typical temperature range monitored during the TDS experiments was between 100 and 860 K. Our other studies have verified that only a few percent of the desorption intensity seen in TDS arises from the back or edges of the crystal (9–12). (This will also be obvious from our results below where we completely cover the front surface with bismuth, but place no Bi on the backs and edges of the crystal.)

In this work, absolute coverages are reported with respect to the number of Pt(111) surface atoms, so that  $\Theta = 1.0$  corresponds to  $1.505 \times 10^{15}$  species  $cm^{-2}$ .

## III. RESULTS

### III.1. Adsorption and Dehydrogenation of $C_6H_{10}$ on Clean Pt(111)

III.1.1. Thermal desorption spectroscopy. A series of thermal desorption spec-

tra from  $C_6H_{10}$  adsorbed on Pt(111) is shown in Figs. 1–3. These figures display the evolution of cyclohexene ( $m/e = 67$ ),  $H_2$  ( $m/e = 2$ ), and benzene ( $m/e = 78$ ) for different exposures of  $C_6H_{10}$  at  $\sim 100$  K. (We abbreviate benzene as simply  $C_6H_6$  throughout this paper.) During these cyclohexene TDS experiments on clean Pt(111), cyclohexadiene, cyclohexane,  $C_2H_2$ ,  $C_2H_4$ , and  $C_2H_6$  were never detected with the mass spectrometer as significant desorption products from the surface.

In Fig. 1 it is possible to observe that for high exposures ( $\geq 1.5$  L) four desorption states of cyclohexene appear in the TDS spectra from  $C_6H_{10}/Pt(111)$ . The presence of these four  $C_6H_{10}$  states desorbing from the front face of the Pt(111) crystal was verified using XPS (see below). The temperatures for the desorption states of  $C_6H_{10}$  are  $\alpha = \sim 158$  K,  $\beta = \sim 190$  K,  $\gamma = \sim 255$  K, and

$\lambda = \sim 300$  K. The desorption temperature of the  $\lambda$ -state is close to that ( $\sim 305$  K) observed for molecular desorption of cyclopentene from Pt(111) (11) but much higher than that for alkanes ( $\sim 236$  K) such as cyclohexane (10). Thus, we can tentatively assign the  $\lambda$ -state to desorption of cyclohexene di- $\sigma$ -bonded to the Pt surface through the two carbon atoms that made up the C–C double bond, as was the case with cyclopentene (11). The similarity in desorption temperatures of the  $\gamma$ -state and that of the first monolayer of cyclohexane adsorbed on Pt(111) ( $\sim 236$  K) (10) suggests that the  $\gamma$ -state corresponds to  $C_6H_{10}$  chemisorbed on Pt(111) through the aliphatic hydrogens (sometimes called agostic bonding), as was the case with adsorbed cyclohexane (10). The  $\alpha$ -state can be assigned to the desorption of the  $C_6H_{10}$  multilayer since it grows continuously with

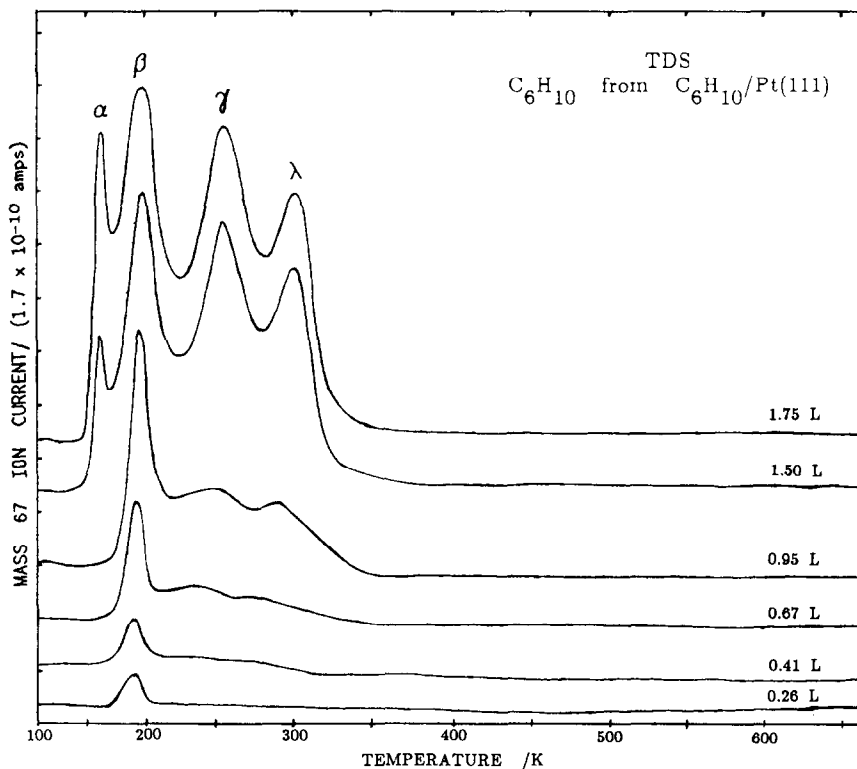


FIG. 1. Thermal desorption spectra showing the evolution of cyclohexene following various  $C_6H_{10}$  exposures to clean Pt(111) at  $\sim 100$  K.

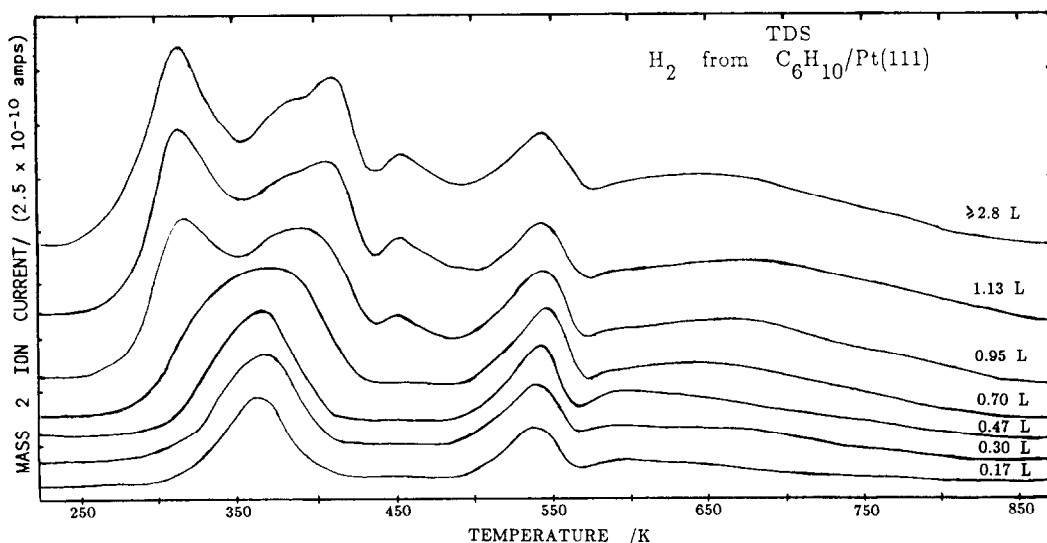
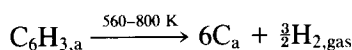
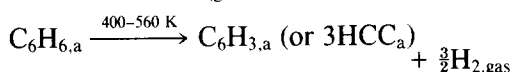
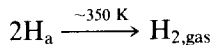
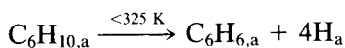


FIG. 2. Thermal desorption spectra showing the evolution of  $H_2$  following various  $C_6H_{10}$  exposures to clean Pt(111) at  $\sim 100$  K.

exposure without saturation. Finally, the  $\beta$ -state will be assigned to desorption of cyclohexene from a state with an adsorption energy between that for cyclohexene bonded directly to Pt(111) and  $C_6H_{10}$  bonded to other  $C_6H_{10}$  molecules. Thus, this "second monolayer" of adsorbed cyclohexene is still close enough to the Pt(111) substrate to feel, partially, its stabilizing influence. Part of this  $\beta$ -peak may also be due to desorption from the backs and edges of the crystal, which are undoubtedly poisoned with an overlayer of carbonaceous residue.

For  $C_6H_{10}$  exposures lower than 0.5 L, the thermal desorption spectra of  $H_2$  evolution (Fig. 2) are characterized by the presence of two clear peaks at 365 and 535 K, and a broad region of desorption between 565 and 805 K. The desorption peak at  $\sim 365$  K is rate-limited by the associative desorption of adsorbed hydrogen atoms ( $2H_a \rightarrow H_2$ ) rather than by C-H bond scission, since this peak is very similar in temperature and shape to that for  $H_2$  desorption from hydrogen adatoms (deposited with  $H_2$  gas) on Pt(111) (14). The higher temperature peaks are rate-limited by rup-

ture of C-H bonds, since they occur well above the normal hydrogen desorption temperature. A quantitative analysis of the area below the spectra in the regions 240–395, 395–565, and 565–810 K showed that these areas are in a ratio of  $(4.2 \pm 0.2) : (2.9 \pm 0.2) : (2.9 \pm 0.2)$  for exposures less than 0.5 L. Such proportions are very close to 4:3:3, which suggests that the  $H_2$  desorption peaks are a consequence of the stoichiometric reactions



Measurements with XPS and AES showed an appreciable amount of adsorbed graphitic carbon after thermal desorption to 860 K (see below), consistent with this mechanism. A very similar sequence of steps was also observed in TDS spectra from cyclohexane on Pt(111) (10). The lineshape of the  $H_2$  TDS spectra observed here between 500 and 810 K is essentially

identical to that reported for adsorbed benzene on Pt(111) (9). As we will see, adsorbed benzene is indeed formed as an intermediate by  $\sim 325$  K in the dehydrogenation of  $C_6H_{10}$  on Pt(111), even at the lowest exposures.

For  $C_6H_{10}$  exposures greater than 1.0 L, the TDS spectra for  $H_2$  evolution (see Fig. 2) show a new lineshape, now with five peaks at 315, 380, 410, 450, and 540 K and a broad region of desorption between 565 and 850 K. Of all these features, only the peak at 315 K could be rate-limited by hydrogen desorption, whereas all the higher-temperature peaks are rate-limited by scission of C-H bonds. (Note that the normal associative  $H_2$  desorption temperature for hydrogen adatoms on Pt(111) decreases from  $\sim 370$  to 300 K with increasing coverage (14).) For high exposures of  $C_6H_{10}$  ( $\geq 1$  L) it is difficult to propose a unique mechanism for dehydrogenation of cyclohexene.

After these large exposures ( $\geq 1$  L) there is a high coverage of  $C_6H_{10}$  on the surface at

$\sim 100$  K. Under these conditions it is expected that most of the free Pt sites necessary for  $C_6H_{10}$  dehydrogenation (i.e., hydrogen abstraction) would be blocked. When the temperature is raised to  $\sim 270$  K in the thermal desorption experiment, part of the  $C_6H_{10}$  molecules desorb (those in the  $\gamma$ -state), leaving vacant sites on the surface which then allow for the dehydrogenation of some of the  $C_6H_{10}$  molecules that are still adsorbed (i.e., the  $\lambda$ -state). At this point, our XPS results below suggest that partial dehydrogenation begins. However, the hydrogen adatoms thus produced do not yet desorb from the surface as can be seen in Fig. 2. In these high-coverage cases, the lack of a sufficient number of empty sites on the surface prevents full dehydrogenation of cyclohexene to produce benzene. By 350 K the chemisorbed hydrogen adatoms and all the remaining adsorbed  $C_6H_{10}$  molecules ( $\lambda$ -state) desorb, leaving new free sites on the surface. The average C:H ratio on the surface at this point was deter-

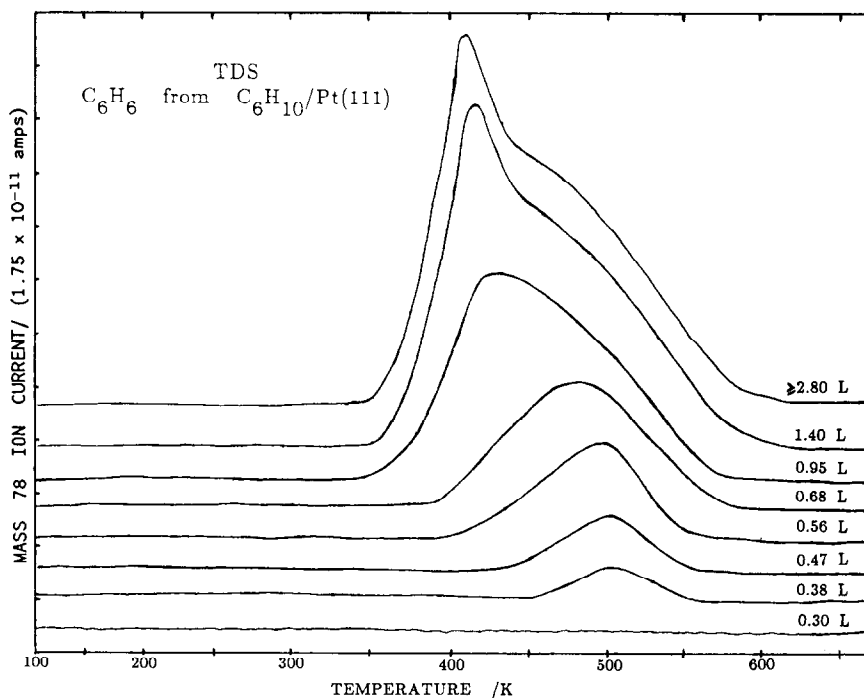


FIG. 3. Thermal desorption spectra showing the evolution of benzene following various  $C_6H_{10}$  exposures to clean Pt(111) at  $\sim 100$  K.

mined to be  $6.0 : 7.5 \pm 0.4$  from quantitative calculations using C(1s) XPS and H<sub>2</sub> TDS peak areas (and relying on the low-coverage data where the stoichiometry is known for calibration). Whereas all the C<sub>6</sub>H<sub>10,a</sub> has desorbed by this temperature, this stoichiometry suggests that the adlayer probably consists of some adsorbed benzene (since it is the only product at this temperature at lower coverages) and at least one other new adsorbed intermediate with stoichiometry between C<sub>6</sub>H<sub>9</sub> and C<sub>6</sub>H<sub>8</sub>. As the temperature increases further, benzene starts to desorb, leaving new free sites. Note that this onset of benzene desorption corresponds exactly with a new increase in H<sub>2</sub> evolution rate, which suggests that these fresh Pt sites are utilized by the new hydrocarbon intermediate for further dehydrogenation. This dehydrogenation gives rise to the peak at 410 K in the H<sub>2</sub> TDS, which is coincident with a sharp peak in the benzene TDS spectrum (see Fig. 3). It is interesting to note that this benzene TDS peak is much sharper and also more intense than that in the benzene TDS spectrum obtained by dosing benzene itself to Pt(111) (9). This implies an autocatalytic mechanism whereby benzene desorption creates new sites for further benzene production by dehydrogenation of the above-mentioned new intermediate. This benzene is then itself available for desorption. The H<sub>2</sub> peak at ~540 K and the broad region of desorption between 565 and 850 K observed in the H<sub>2</sub> TDS spectra for exposures greater than 1.0 L are due to decomposition of adsorbed benzene, and these show almost the same lineshape as that at lower coverages of cyclohexene or from dosing pure benzene to Pt(111) (9).

Thermal desorption spectra for C<sub>6</sub>H<sub>6</sub> evolution from C<sub>6</sub>H<sub>10</sub>/Pt(111) are displayed in Fig. 3. In these spectra the range of desorption temperatures is similar to that observed for desorption of benzene from C<sub>6</sub>H<sub>6</sub>/Pt(111) (see Ref. 9, Fig. 3). During the experiments on the clean Pt(111) surface for exposures lower than 0.30 L, no significant amount of benzene was ob-

served to desorb from the surface in TDS. This is due to the fact that the amount of benzene formed from cyclohexene in this exposure range is relatively small ( $\Theta_{\text{C}_6\text{H}_6} < 0.07$ , see below) and it all decomposes on the surface during further heating. For benzene adsorbed on clean Pt(111), no molecular desorption is reported for  $\Theta_{\text{C}_6\text{H}_6} < 0.07$  (9). In those cases, adsorbed benzene entirely decomposes to liberate H<sub>2</sub>. The reason that adsorbed benzene desorbs intact at high coverage but entirely dehydrogenates at low coverage is that, at high coverage, no free Pt sites remain on the surface for abstraction of hydrogen atoms (9). As we see in Section III.3, we were able to confirm the presence of adsorbed benzene as a dehydrogenation product even at the lowest exposures of C<sub>6</sub>H<sub>10</sub> ( $\leq 0.3$  L), by *postdosing* a cyclohexene adlayer that had been heated to 360 K with Bi to prevent further dehydrogenation of the C<sub>6</sub>H<sub>6</sub> species during TDS.

Figure 4 shows the uptake curve for cyclohexene on clean Pt(111). The figure displays the variation in the amounts of the four molecular desorption states of C<sub>6</sub>H<sub>10</sub> ( $\alpha$ ,  $\beta$ ,  $\gamma$ , and  $\lambda$ ) with exposure. For C<sub>6</sub>H<sub>10</sub> exposures smaller than 3 L, this dependence was directly obtained from the areas in the TDS spectra, scaled to absolute coverage units using the calibrated ratio of carbon-platinum XPS areas (see below). For C<sub>6</sub>H<sub>10</sub> exposures higher than 3 L, employing quantitative XPS as a function of flash temperature (see below), we found that the  $\beta$ -,  $\gamma$ -, and  $\lambda$ -state saturate and that the  $\alpha$ -state (multilayer) grows continuously. We have used this result to extrapolate the curves to above 3 L in Fig. 4. (For exposures above 3 L, all the molecular TDS peak areas falsely appeared to grow with exposure due to an ever-increasing tail on the multilayer TDS peak, caused by the very slow pumping speed of cyclohexene.) In Fig. 4, the "C<sub>6</sub>H<sub>6</sub>" curve represents the variation of the amount of benzene which evolves during TDS as a function of the exposure. The curve was obtained directly us-

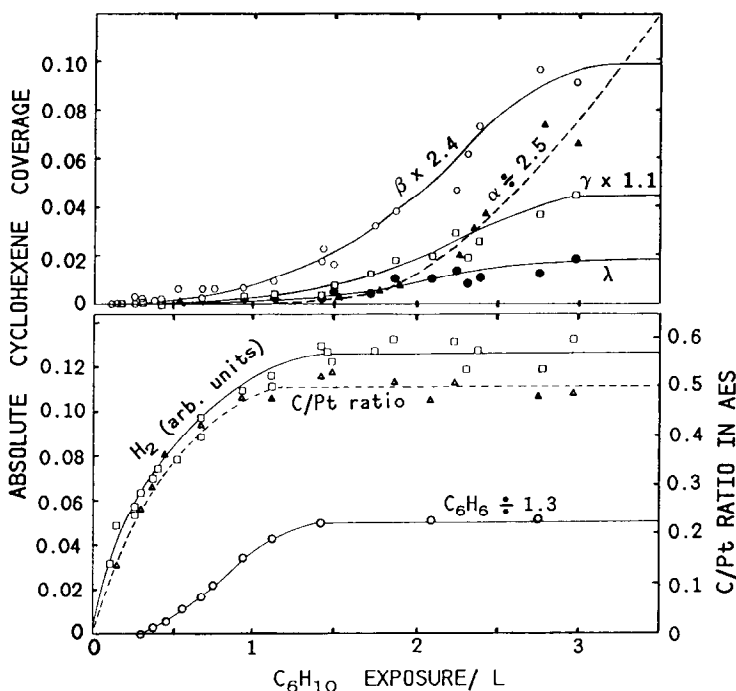


FIG. 4. Variation of the areas of different desorption states or amounts of the desorption states seen in TDS with cyclohexene exposure to Pt(111) at 100 K. Also shown is the C(272)/Pt(237) peak-to-peak AES ratio obtained after TDS to 850 K. All curves (except  $H_2$ ) were scaled to equivalent absolute coverages of cyclohexene as described in text.

ing the area below the  $C_6H_6$  thermal desorption spectra and was scaled with respect to the other curves using the difference in calibrated ratio of carbon-platinum XPS areas before and after benzene desorption (see below). The " $H_2$ " curve (in arbitrary units) shows the total area of desorbed  $H_2$  during TDS as a function of exposure. Finally, the "C/Pt" curve displays the variation in the amount of carbon residue on the surface measured by the C(272)/Pt(237) peak-to-peak ratio in the AES spectra taken after heating to  $\sim 850$  K in the thermal desorption experiments. Using XPS data (see below) the "C/Pt" curve was scaled in such a way that it also represents the absolute coverage of cyclohexene which totally decomposes on the surface to produce adsorbed carbon.

As can be seen in Fig. 4,  $C_6H_{10}$  dehydrogenation predominates at the lowest exposures and saturates at  $\sim 1.5$  L. Below 0.2 L, the ratio of the amount of  $C_6H_{10}$  which de-

hydrogenates to that which desorbs molecularly is at least 50, which can be taken as a lower limit on the ratio of rate constants for dehydrogenation:desorption on clean Pt(111) at the desorption temperature (300 K). By  $\sim 0.3$  L, benzene desorption starts to grow, saturating at  $\sim 1.4$  L. The  $\beta$ -,  $\gamma$ -, and  $\lambda$ -peaks for cyclohexene desorption grow almost simultaneously (see Fig. 1) starting from  $\sim 0.4$  L but accelerating after saturation of the dehydrogenation curves. These peaks saturate at  $\sim 3$  L exposure, after which the  $\alpha$  (multilayer)-peak grows without saturation. The order of appearance of the  $\beta$ -,  $\gamma$ -, and  $\lambda$ -peaks is *not* what is usually expected, where the most strongly bound states populate first and their TDS peaks appear first with increasing exposure. The molecules adsorbed in the  $\lambda$ -state have a larger desorption temperature and, therefore, a much higher probability of being dehydrogenated than the molecules in

the  $\beta$ -, and  $\gamma$ -states since dehydrogenation is a thermally activated process. Most of the  $\lambda$ -state molecules will therefore not appear in the molecular desorption peak since they instead dehydrogenate. Note, for example, the situation in Fig. 4, at  $\sim 1$  L exposure. Of the total cyclohexene coverage of 0.16 molecule per Pt atom, about 97% dehydrogenate to produce benzene or carbon residue during TDS and only  $\sim 3.5\%$  desorb molecularly. Thus, almost all the molecules were probably originally bonded in the high-temperature  $\lambda$ -state, but most of these did not appear in the  $\lambda$ -TDS peak due to competition from the dehydrogenation pathway. Thus, the order of the  $\beta$ -,  $\gamma$ -, and  $\lambda$ -peaks in the  $C_6H_{10}$  TDS spectra does not have any direct implication about the order of population of the corresponding states on the Pt(111) surface.

It can be seen in Fig. 4 that there is a notable growing of the  $\lambda$ -state for  $C_6H_{10}$  molecular desorption only after saturation of the curves for dehydrogenation and benzene evolution ( $\sim 1.4$  L). Once the Pt sites start to be largely covered by adsorbed species, desorption of  $C_6H_{10}$  becomes possible due to the lack of empty sites for dehydrogenation. For an exposure which just saturates the  $\gamma$ - and  $\lambda$ -states (3 L), we found that approximately three of every four molecules that are adsorbed on the Pt surface dehydrogenate during TDS. If all of these molecules which dehydrogenate are originally in the  $\lambda$ -state as we expect, then the maximum coverages of the  $\gamma$ - and  $\beta$ -states are each only  $\sim 22\%$  of the  $\lambda$ -state.

On the basis of the variation of the total amount of chemisorbed cyclohexene with exposure, we were able to determine the sticking coefficient of  $C_6H_{10}$  on a clean Pt(111) surface at 100 K. (The gas temperature was 300 K.) The value was 0.21. This value is very similar to the values reported for other  $C_5$ – $C_6$  hydrocarbons on Pt(111) and discussed elsewhere (10).

*III.1.2. X-ray photoelectron spectroscopy.* Curve (a) of Fig. 5 displays the  $C(1s)$  X-ray photoelectron spectrum after dosing

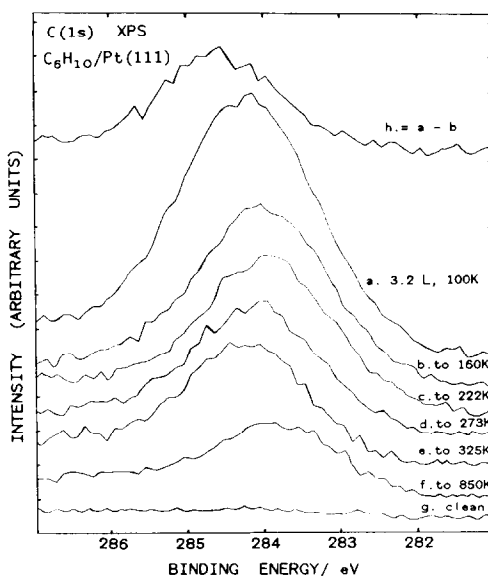


FIG. 5.  $C(1s)$  XPS spectrum following cyclohexene adsorption on clean Pt(111): (a) after dosing 3.2 L of  $C_6H_{10}$  at  $\sim 100$  K; (b) after flashing to 160 K to remove the  $\alpha$ - $C_6H_{10}$  state (multilayer); (c) after flashing to 222 K to remove the  $\beta$ - $C_6H_{10}$  state (second monolayer); (d) after flashing to 273 K to desorb the  $\gamma$ - $C_6H_{10}$  state; (e) after flashing to 325 K to remove the  $\lambda$ - $C_6H_{10}$  state; (f) after flashing to 850 K to desorb benzene and produce graphitic carbon on the surface; (g) clean surface; and (h) difference spectrum (a – b) representing the  $C(1s)$  spectrum of multilayer cyclohexene alone.

3.2 L of cyclohexene onto the clean Pt(111) surface at  $\sim 100$  K. This dose is sufficient to saturate the  $H_2$ ,  $C_6H_6$ ,  $\beta$ - $C_6H_{10}$ ,  $\gamma$ - $C_6H_{10}$ , and  $\lambda$ - $C_6H_{10}$  TDS peaks and to populate the equivalent of about two-thirds of a monolayer of the multilayer state. Curves (b)–(f) show spectra obtained by briefly flashing this overlayer to the indicated upper temperature limits to desorb the different individual adsorption states. Note that there are not huge differences in the position of the  $C(1s)$  peak as successively higher temperature states are desorbed. The peaks always appear in the range between 283.8 to 284.6 eV.

The difference spectrum of curve (a) minus (b) in Fig. 5, which reflects the cyclohexene multilayer, is shown as curve (h). It is centered at 284.6 eV. Curve (c), which reflects the saturated monolayer ( $\gamma$ - and  $\lambda$ -



states) remaining *after* heating to 222 K to desorb the multilayer and  $\beta$ -states, is centered at 283.8 eV. This energy position is within the range of values ( $283.6 \pm 0.2$  eV) reported for  $sp^3$ -hybridized carbon atoms in small hydrocarbons adsorbed on Pt(111) (11), suggesting that  $sp^3$ -type carbon dominates on the surface at this point. Upon heating to 273 K, the cyclohexene adsorbed in the  $\gamma$ -state desorbs and a C(1s) peak centered at 284.0 eV remains (curve (d)). Further heating to 325 K to desorb the  $\lambda$ -state of adsorbed  $C_6H_{10}$  leaves a C(1s) peak now centered at 284.2 eV (curve (e)). This peak position is very close to the value of 284.32 eV reported in our previous work (9) for molecularly adsorbed benzene on clean Pt(111), and within the range ( $284.2 \pm 0.1$  eV) reported for  $sp^2$ -hybridized carbon atoms in small hydrocarbons on Pt(111) (11). This suggests that  $sp^2$ -type carbon atoms dominate on the surface here. For the conditions under which spectrum (e) was taken, it is likely that benzene is coadsorbed on the Pt surface with another cyclic hydrocarbon(s) of composition between  $C_6H_{10}$  and  $C_6H_8$  (see above). Finally, heating the surface to 850 K (i.e., the completion of  $H_2$  evolution) leaves a C(1s) peak centered at 283.8 eV (curve (f)). This is the exact position reported in the literature (9) for the extended graphitic residue remaining on Pt(111) after complete dehydrogenation of adsorbed benzene and other hydrocarbons. The fact that the C(1s) peak obtained after flashing to 273 K is at 284.0 eV, midway between the ranges expected for  $sp^2$ - and  $sp^3$ -type hydrocarbons, suggests that a mixture of both types of carbons exists in the adlayer at 273 K. The peak width (FWHM) for this spectrum of 1.85 eV is slightly larger than the overall instrumental resolution ( $\sim 1.65$  eV), also consistent with a mixture of species. Since the carbon was mostly  $sp^3$ -hybridized at 222 K, this suggests that some partial dehydrogenation has already occurred by 273 K, before any  $H_2$  evolution.

Experiments such as that shown in Fig. 5

were repeated a number of times for initial cyclohexene exposures exceeding 3 L, which were sufficient to saturate the  $\beta$ -,  $\gamma$ -, and  $\lambda$ -molecular desorption states of  $C_6H_{10}$  and all the  $H_2$  and  $C_6H_6$  peaks. For these experiments, the average integrated C(1s):Pt(4f) intensity ratio after flashing to 222 K to remove the multilayer and  $\beta$ -desorption states was  $0.0183 \pm 0.0007$ . This reflects the saturation coverage of molecularly adsorbed cyclohexene on Pt(111). The C/Pt XPS ratios can be scaled to absolute coverage units using the value of  $0.00779 \pm 0.0001$  for this ratio measured in this same instrument for saturation CO exposure at 260 K on Pt(111), which is known to give an absolute CO coverage of  $0.58 \pm 0.02$  (per Pt surface atom) (15). Thus, the saturation (monolayer) coverage of molecularly adsorbed cyclohexene on Pt(111) ( $\gamma$ - plus  $\lambda$ -states, including that which dehydrogenates) is  $0.23 \pm 0.01$  molecule per Pt surface atom. Using the same procedure and differences in the average C/Pt XPS ratios between spectra such as that in Fig. 5 (curves (a) to (f)), we were able to obtain the saturation coverage of the  $\beta$ -state ( $\Theta_{\beta-C_6H_{10}} = 0.04$ ), the maximum amount of  $C_6H_{10}$  that desorbs in the  $\gamma$  ( $\Theta_{\gamma-C_6H_{10}} = 0.04$ ) and  $\lambda$ -states ( $\Theta_{\lambda-C_6H_6} = 0.02$ ), the highest coverage of  $C_6H_{10}$  molecules that dehydrogenate on the surface and remain after flashing to 325 K ( $\Theta_{C_6H_{10}} = 0.17$ ), the maximum amount of benzene that desorbs ( $\Theta_{C_6H_6} = 0.06$ ), and the maximum amount of cyclohexene that completely dehydrogenates and remains as carbon residue at 840 K ( $\Theta_{C_6H_{10}} = 0.11$  or  $\Theta_C = 0.66$ ). Support for the accuracy of this method of absolute coverage calibration for adsorbed hydrocarbons is presented elsewhere (9-11).

These absolute saturation coverages obtained above from XPS results were used as scaling factors for TDS data such as those shown in Figs. 1 to 3. Thus, for example, the saturation  $C_6H_{10}$  TDS peak areas of the  $\beta$ -,  $\gamma$ -, and  $\lambda$ -states correspond to absolute cyclohexene coverages of 0.04, 0.04, and 0.02, respectively. The scaling factors ob-

tained in this way were used to convert TDS peak areas to absolute coverage units in Fig. 4 and throughout this paper. These XPS data were also employed to scale the C(272)/Pt(237) peak-to-peak ratio in the AES spectra of graphitic residue to absolute cyclohexene coverage. Saturation of the residual C/Pt AES ratio in Fig. 4 corresponds to a cyclohexene coverage of 0.11 (the maximum coverage that completely dehydrogenates on the surface).

### II.2. Adsorption and Dehydrogenation of $C_6H_{10}$ on Bismuth-Covered Pt(111)

One main objective of this work is to measure the number of active sites on the surface which are required for dehydrogenation of  $C_6H_{10}$  on Pt(111). To address this issue, we first vapor-deposited Bi on the surface at  $<125$  K, then dosed cyclohexene at  $\sim 100$  K, and finally observed the changes in the TDS peaks and corresponding reaction rates as the concentration of the Bi overlayer increased.

The adsorption and growth modes of Bi on Pt(111) have been discussed in detail previously (16). There are weakly repulsive Bi-Bi interactions in the adlayer which cause the Bi adatoms to spread uniformly across the surface, probably sitting in three-fold hollow sites for absolute coverages below one-third. For absolute coverages below 0.25 ( $\Theta_{Bi}^* = 0.45$ ), no LEED patterns are observable above 100 K and the Bi adatoms are thought to be nearly randomly spread across the surface. A close-packed monolayer of Bi on Pt(111) corresponds to an absolute coverage of 0.56. Our Bi coverages here will be reported relative to that value. We will refer to these scaled coverages as  $\Theta_{Bi}^*$ ; and they thus refer to the fraction of a close-packed monolayer. For all the results presented in this section, the Bi was first deposited on the clean surface (at a temperature  $<125$  K); after that, a dose of cyclohexene was given to the bismuth-covered Pt surface, and then the XPS and TDS experiments were carried out. The Bi coverages were determined using Bi/Pt XPS

peak ratios, calibrated as described previously (9). They were generally measured immediately after deposition of Bi, but for submonolayer coverages they remained constant throughout the TDS up to 820 K.

*III.2.1. Thermal desorption spectroscopy.* Figures 6 to 8 display the effect of Bi precoverage on the  $H_2$  ( $m/e = 2$ ),  $C_6H_{10}$  ( $m/e = 67$ ), and  $C_6H_6$  ( $m/e = 78$ ) TDS spectra for a fixed  $C_6H_{10}$  exposure of 0.28 L at  $\sim 100$  K. On a clean Pt(111) surface this exposure leads to an initial cyclohexene coverage of  $\sim 0.06$  molecule per Pt atom. As discussed above with respect to TDS from the clean Pt(111) surface, almost all of the adsorbed  $C_6H_{10}$  dehydrogenates upon heating to 400 K to produce adsorbed benzene at this exposure, and this benzene itself totally decomposes on the surface to leave graphitic residue by 840 K. The very small amount of molecular desorption in the absence of Bi, seen only in the  $\beta$ -peak, is probably due to minor background desorption from the backs and edges of the crystal.

As Bi is added, Fig. 6 shows that  $H_2$  evolution is almost completely suppressed by  $\Theta_{Bi}^* = 0.5$ . The  $H_2$  intensity in the region for dehydrogenation of adsorbed benzene ( $T > 500$  K) decreases monotonically with increasing Bi precoverage and has almost disappeared by  $\Theta_{Bi}^* = 0.20$ . This coincides with an increase in the amount of benzene desorbing molecularly from the surface (see Fig. 7,  $\Theta_{Bi}^* < 0.2$ ). This increase in molecular desorption of benzene occurs over the same Bi coverage range as was seen in benzene/Bi coadsorption experiments on Pt(111) (9). It was attributed to the fact that the dehydrogenation pathway for adsorbed benzene is almost completely blocked by Bi adatoms at  $\Theta_{Bi}^* = 0.2$  via an ensemble effect, and the  $C_6H_6$  molecule is now obliged to desorb (9).

Inspection of the region below 500 K in Fig. 6 shows a complete change in the  $H_2$  TDS peak structure as Bi is added. This suggests that there may be a change in the mechanism of dehydrogenation of  $C_6H_{10}$  (or

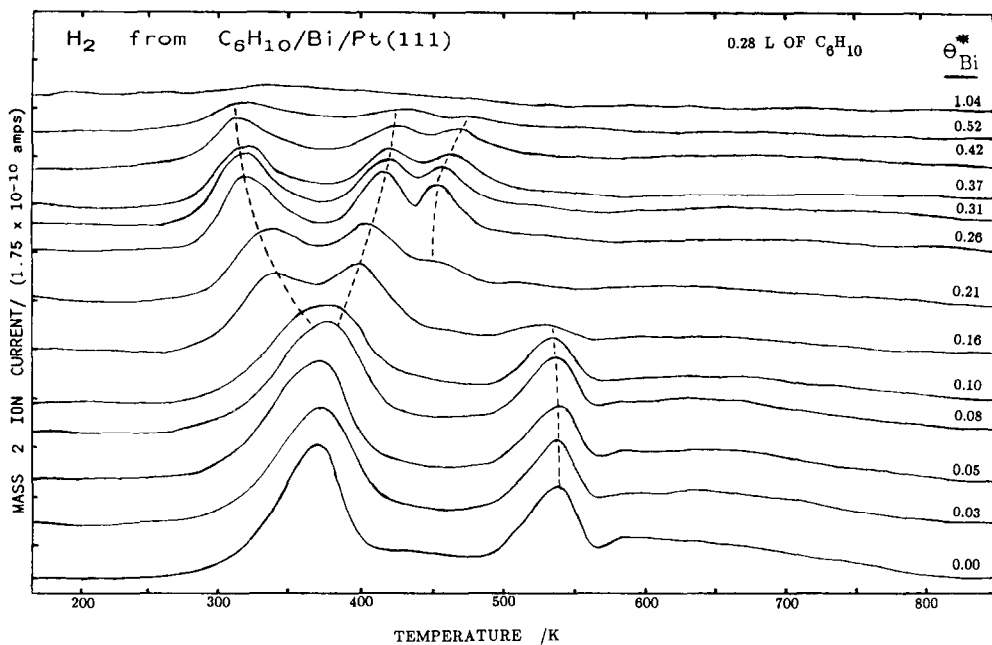


FIG. 6. Effect of Bi pre dosing on the dehydrogenation of  $C_6H_{10}$  on Pt(111): variation in  $H_2$  TDS spectra with  $\Theta_{Bi}^*$  for a fixed  $C_6H_{10}$  exposure of 0.28 L at  $\sim 100$  K.

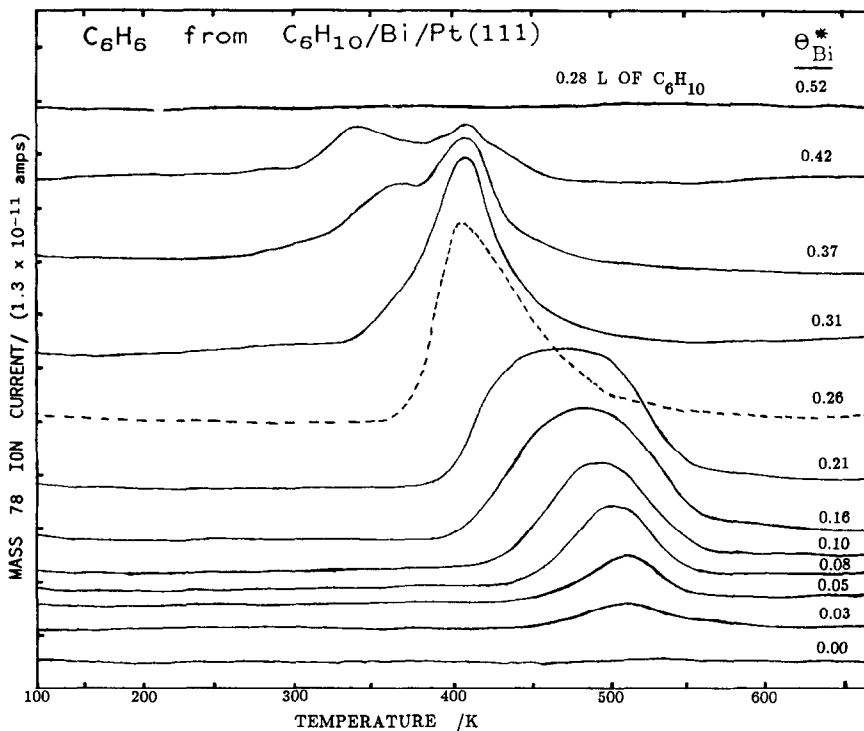


FIG. 7. Effect of Bi pre dosing on the dehydrogenation of  $C_6H_{10}$  on Pt(111): variation in benzene TDS spectra with  $\Theta_{Bi}^*$  for a fixed  $C_6H_{10}$  exposure of 0.28 L at  $\sim 100$  K.

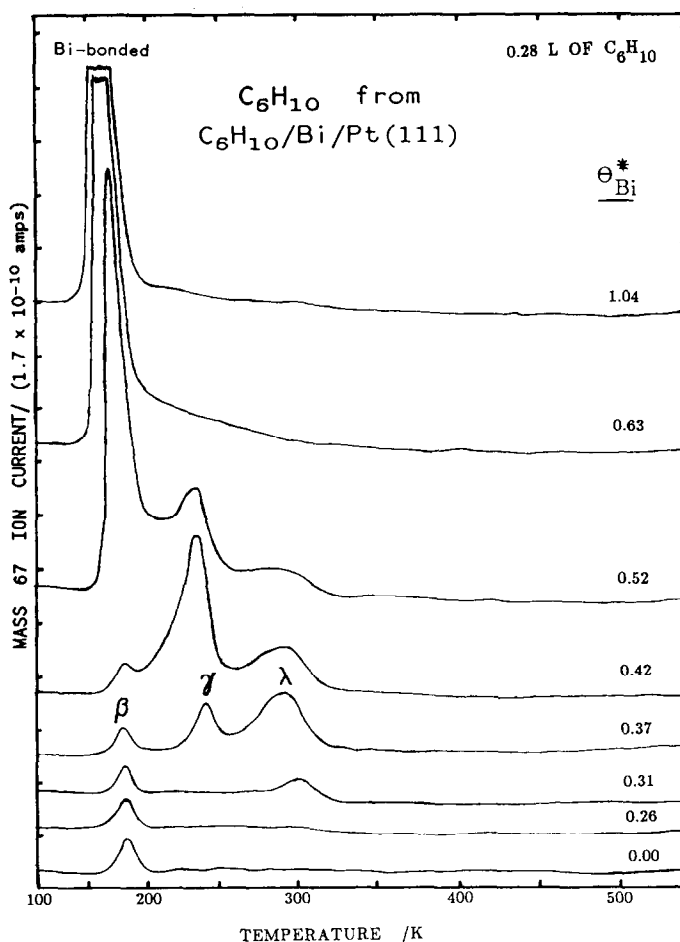


FIG. 8. Effect of Bi pre dosing on the dehydrogenation of  $C_6H_{10}$  on Pt(111): variation in molecular  $C_6H_{10}$  TDS spectra with  $\Theta_{Bi}^*$  for a fixed  $C_6H_{10}$  exposure of 0.28 L at  $\sim 100$  K.

at least in the stability of partially dehydrogenated intermediates) as a function of Bi precoverage, just as occurred in the absence of Bi with increasing cyclohexene coverages (see above). The  $H_2$  TDS peak at  $\sim 370$  K in the absence of Bi is desorption rate-limited and occurs at the same temperature as normal hydrogen desorption on clean Pt(111) for low hydrogen coverages. As  $\Theta_{Bi}^*$  increases, this peak decreases in intensity and eventually splits into two and then three peaks. The lowest temperature peak occurs at  $\sim 310$  K for  $\Theta_{Bi}^* \geq 0.2$ , which is identical to the normal hydrogen desorption temperature at this bismuth coverage (11, 24). This 310 K peak is therefore also

hydrogen desorption rate-limited, but now the two higher-temperature peaks ( $\sim 425$  and  $465$  K) are rate-limited by C–H bond cleavage instead. At  $\sim 350$  K (i.e., after completion of the hydrogen desorption-limited peak), the stoichiometry of the surface was determined to be C : H  $\approx 6 : 8.4$  for  $\Theta_{Bi}^* = 0.26$ . Since cyclohexene desorption is completed already at lower temperatures, no cyclohexene remains adsorbed. This suggests that, as with high cyclohexene coverages, high Bi coverages stabilize a new intermediate with stoichiometry of approximately  $C_6H_9$ , which probably coexists with small amounts of adsorbed benzene. It is likely that, while adsorbed benzene is the

thermodynamically stable product of cyclohexene dehydrogenation, a less stable, partially dehydrogenated intermediate can be stabilized at high concentrations when no more free Pt sites exist for further hydrogen abstraction. This intermediate must have a desorption temperature above that of benzene, since it is never evolved into the gas phase. Due to the similarities in their  $H_2$  TDS lineshapes, it is likely that the reaction pathway for  $C_6H_{10}$  dehydrogenation at high Bi precoverage is similar to that observed for  $C_6H_{10}$  dehydrogenation on clean Pt(111) at large coverages of  $C_6H_{10}$  (see Section III.1.1). Again, the onset of the  $H_2$  TDS peak at  $\sim 400$  K is simultaneous with the onset of benzene desorption (compare Figs. 6 and 7 at  $\Theta_{Bi}^* = 0.26$  and  $0.31$ ). This is consistent with a common rate-determining step here. Again, benzene desorption is probably creating free sites, which then allow further dehydrogenation of the new intermediate.

The shift toward lower temperatures of the benzene TDS peaks with increasing Bi precoverage, observed in Fig. 7, is very similar to that reported and discussed previously (9) for benzene and Bi coadsorption on Pt(111) surfaces.

Figure 8 displays the effect of Bi precoverage on the TDS spectrum of molecularly desorbing cyclohexene. For  $\Theta_{Bi}^* < 0.25$  only background desorption from the  $\beta$ -state is observed. With increasing  $\Theta_{Bi}^*$ , first the  $\lambda$ -peak for di- $\sigma$ -bonded  $C_6H_{10}$  grows and then decays, after which the  $\gamma$ -peak for agostically bonded  $C_6H_{10}$  grows and then decays. Finally, all the cyclohexene desorbs in a single peak at  $\sim 170$  K for Bi coverages approaching a monolayer. The growth of the  $\lambda$ -state prior to the  $\gamma$ -state in Fig. 8 is consistent with a model whereby the  $\lambda$ -state is mainly responsible for dehydrogenation, and so it grows as dehydrogenation is killed by the addition of Bi. Only after there are no more sites available for the more stable  $\lambda$ -state does the  $\gamma$ -state grow. For high coverages of Bi ( $\Theta_{Bi}^* \geq 0.7$ ), the low desorption temperature (170 K) suggests that the cyclohexene molecules are bonded above the

Bi adlayer, bound only to Bi atoms and not to Pt atoms. By comparison to Fig. 1, we can see that the cyclohexene desorption temperature when  $\Theta_{Bi}^* = 1.0$  is about the same as its multilayer desorption temperatures. At this coverage there is no dehydrogenation (see Fig. 6). The much lower cyclohexene desorption temperature when  $\Theta_{Bi}^*$  exceeds 0.7 compared to clean Pt(111) shows that  $C_6H_{10}$  is much more strongly bonded to the Pt atoms than to the Bi atoms, consistent with the well-known weakness of bismuth/hydrocarbon interactions (7-12). The desorption temperature observed in Fig. 8 for the  $\lambda$ - $C_6H_{10}$  state at  $\Theta_{Bi}^* = 0.31$  is identical to that observed for desorption of this most stably bonded cyclohexene state from clean Pt(111). This fact shows that for  $\Theta_{Bi}^* \leq 0.30$ , any electronic influence of Bi upon the heat of chemisorption of  $C_6H_{10}$  is negligible. Although some electronic influences may be important at higher Bi coverages, it appears that, even there, the major role of Bi is to block sites and thereby force cyclohexene molecules to assume new, less stable adsorption geometries.

Figure 9 summarizes the results of many TDS experiments such as those shown in the representative spectra of Figs. 6 to 8. Here we show the effect of Bi precoverage on the various TDS peak areas and on the total probability for cyclohexene dehydrogenation (taken as 1.0 minus its molecular desorption probability). At first ( $\Theta_{Bi}^* < 0.3$ ), the probability of cyclohexene dehydrogenation remains nearly constant at unity, although the amount of benzene desorption increases due to the fact that Bi is blocking sites necessary for the further dehydrogenation of benzene. This shows that benzene dehydrogenation has a larger effective ensemble requirement than cyclohexene dehydrogenation. As  $\Theta_{Bi}^*$  increases further ( $\Theta_{Bi}^* > 0.3$ ), the dehydrogenation probability for cyclohexene finally starts to decrease and dies by  $\Theta_{Bi}^* = 0.6$ . Since benzene (plus  $H_2$ ) is the only ultimate product of cyclohexene dehydrogenation in this coverage region, the benzene TDS peak area cor-

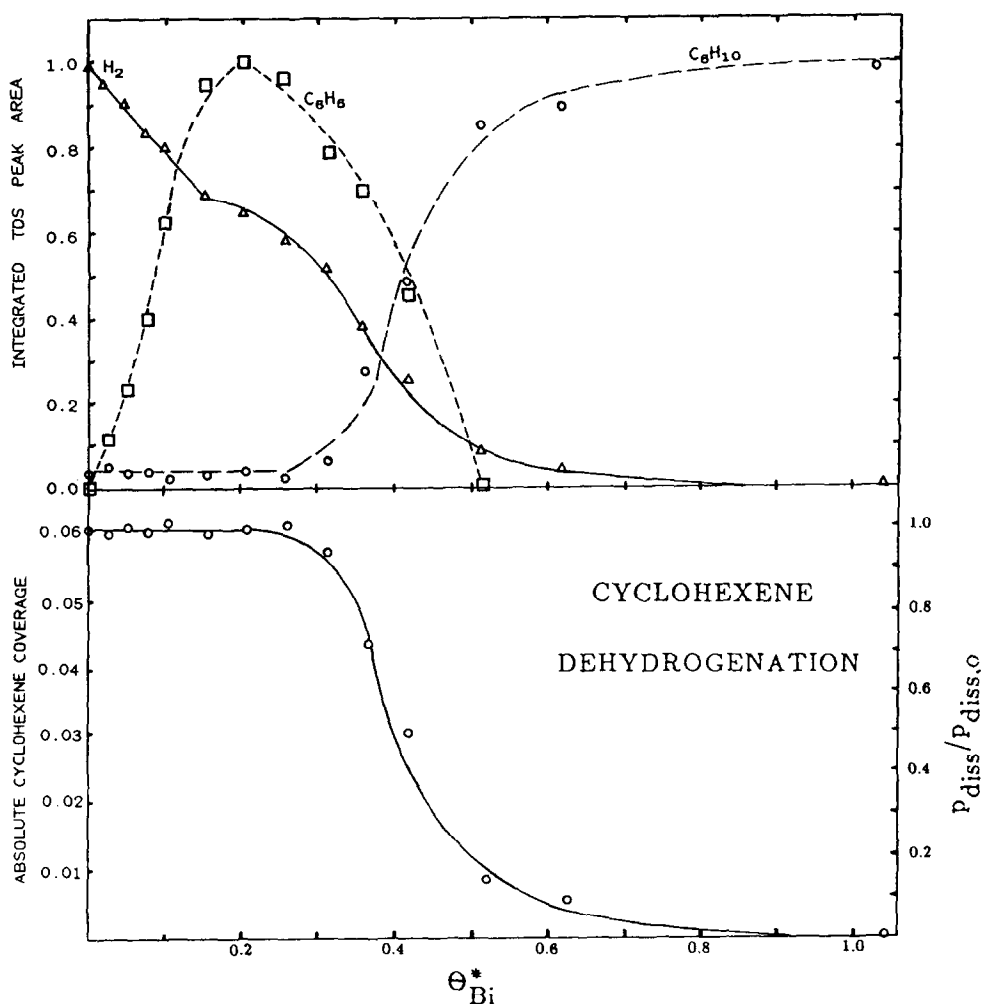


FIG. 9. Variation in the amounts of desorption products and dehydrogenation of cyclohexene versus bismuth precoverage for a 0.28 L dose of cyclohexene at  $\sim 100$  K on Pt(111). The top part of this figure shows the variation of the integrated TDS peak areas for the total amounts of  $H_2$ , benzene, and cyclohexene evolution (exemplified by the representative data in Figs. 6–8) with  $\Theta_{Bi}^*$ . The bottom part of this figure was obtained by taking one minus the relative cyclohexene ( $m/e = 67$ ) TDS peak area. This was scaled to absolute coverage units employing the XPS intensities as described in the text. On the right axis,  $P_{diss}$  refers to the probability for dehydrogenation of adsorbed  $C_6H_{10}$  during TDS, and  $P_{diss,0}$  refers to this value ( $\sim 1.0$ ) at zero Bi coverage.

respondingly decreases, directly reflecting the decrease in cyclohexene dehydrogenation probability.

**III.2.2. X-ray photoelectron spectroscopy.** Figure 10 displays typical  $C(1s)$  X-ray photoelectron spectra after dosing 0.2 L of cyclohexene ( $\Theta_{C_6H_{10}} = 0.04$ ) onto the Pt surface which had been predosed with various Bi coverages. Curves (a) to (e) were taken immediately after dosing  $C_6H_{10}$  at  $\sim 100$  K.

Comparison of these curves shows that there is a smooth increase of  $\sim 1.2$  eV in the  $C(1s)$  binding energy of adsorbed cyclohexene as  $\Theta_{Bi}^*$  increases in the first monolayer. This total decrease is similar in magnitude to the Bi-induced work function decrease. It is an indication of the difference between the Pt-bound and the Bi-bound cyclohexene. The reason for the increase in binding energy is explained in a separate paper (10)

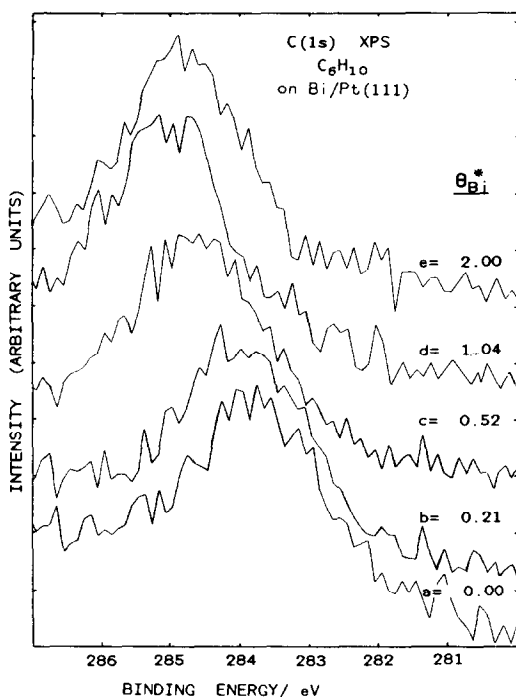


FIG. 10. Effect of Bi predosing upon the C(1s) XPS spectra of cyclohexene adsorbed on Bi-covered Pt(111). Spectra were taken after dosing 0.2 L of  $C_6H_{10}$  onto the surface at  $\sim 100$  K containing various Bi coverages.

using a model similar to that used by Wandelt to explain the photoemission of adsorbed xenon (PAX) (17).

Using C(1s) XPS intensities versus exposure, we were able to determine that for low exposures of  $C_6H_{10}$  the sticking coefficient of cyclohexene at 100 K is approximately independent of Bi precoverage.

### III.3. Bismuth Postdosing Thermal Desorption Mass Spectroscopy (BPTDS)

The TDS spectra following exposures of cyclohexene lower than 0.3 L to clean Pt(111) suggested that an intermediate of stoichiometry  $C_6H_6$ , perhaps benzene, might be on the surface between  $\sim 350$  and 400 K. To test this, we postdosed bismuth to a Pt(111) surface which had previously been exposed to 0.28 L of cyclohexene and which had been heated to 360 K to remove

hydrogen and produce a surface containing only the suspected benzene intermediate. The hope here was that the Bi adatoms might block the Pt sites necessary for  $C_6H_6$  dehydrogenation during subsequent heating and allow the molecular desorption of benzene and its identification by mass spectroscopy. Figure 11 shows the  $H_2$  ( $m/e = 2$ ) and  $C_6H_6$  ( $m/e = 78$ ) TDS spectra for a 0.28 L  $C_6H_{10}$  exposure onto clean Pt(111) at  $\sim 100$  K which had been flashed briefly to 360 K and then postdosed with various Bi coverages at  $\sim 110$  K. With no Bi, only  $H_2$  is liberated in TDS. The  $H_2$  TDS peaks are uniformly attenuated with increasing Bi postcoverage and benzene desorption appears and grows. By  $\Theta_{Bi}^* = 0.5$ , the dehydrogenation ( $H_2$  TDS) is completely suppressed, and there is very strong benzene desorption. Inspection of this surface after the TDS up to temperatures of  $\sim 850$  K using XPS and AES showed no observable carbon residue, a fact consistent with the complete suppression of dehydrogenation by the postdosed Bi.

In Fig. 11, for  $\Theta_{Bi}^* < 0.21$ , the desorption temperature for  $C_6H_6$  and its TDS lineshape are similar to those following intermediate exposures of benzene to clean Pt(111) (9). The shift of the molecular benzene desorption peak to lower temperatures at higher Bi postcoverages, as seen in Fig. 11, was also observed in predosing Bi with benzene exposures (9) and when adsorbed benzene is generated on a Bi predosed surface (Fig. 7).

The dependence of the  $H_2$  and  $C_6H_6$  TDS peak areas upon the Bi postdose coverage is shown in Fig. 12. This figure shows a dependence upon  $\Theta_{Bi}^*$  which is similar to that reported in another study (9) where Bi was predosed and then benzene was dosed to Pt(111). This confirms that (i) the adsorbed species produced from the dehydrogenation of cyclohexene at low exposures on Pt(111) is indeed adsorbed benzene, and (ii) the vapor deposition of Bi onto a  $C_6H_6$ /Pt(111) surface does not damage the benzene adlayer. We refer to the type of exper-

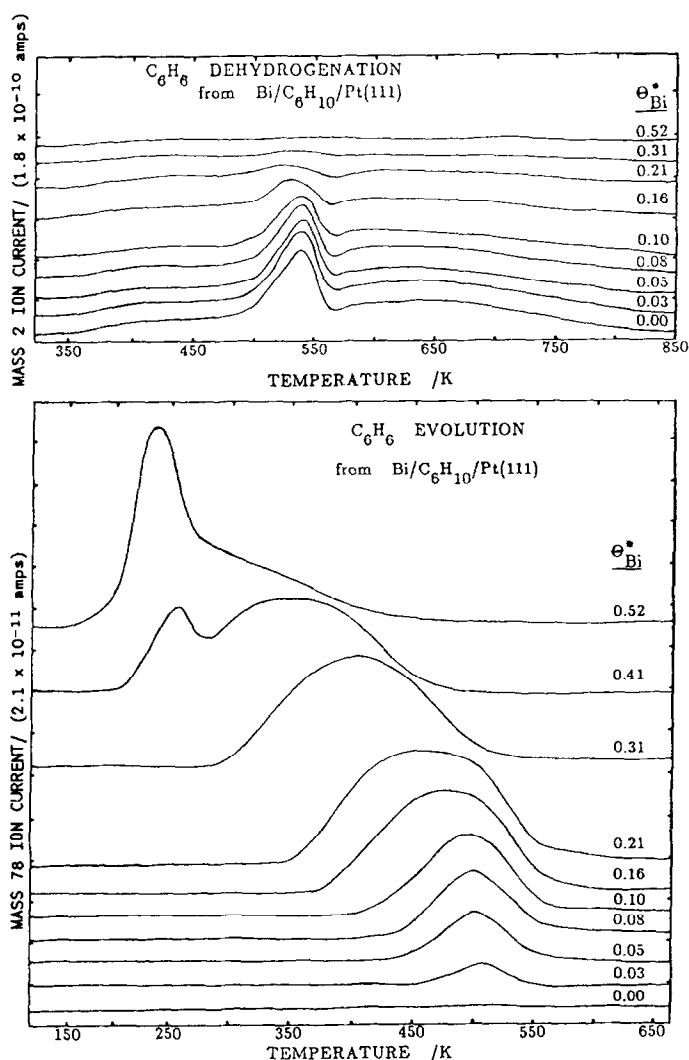


FIG. 11. Variations in  $\text{H}_2$  ( $m/e = 2$ ) and  $\text{C}_6\text{H}_6$  ( $m/e = 78$ ) TDS spectra with Bi postdosed coverage for a fixed cyclohexene exposure of 0.28 L. Cyclohexene was first dosed onto clean Pt(111) at  $\sim 100$  K. The surface was then flashed briefly to 360 K (presumably to produce adsorbed benzene and desorb  $\text{H}_2$ ), and finally postdosed with various Bi coverages at  $\sim 110$  K prior to TDS.

iment described above as "bismuth postdosing in thermal desorption spectroscopy," BPTDS (8).

Attempts were made to use BPTDS to identify the new adsorbed intermediate(s) coproduced with adsorbed benzene during TDS between 350 and 500 K, when  $\text{C}_6\text{H}_{10}$  exposures  $\geq 1$  L are given to a clean Pt(111) surface, or from lower exposures when  $\Theta_{\text{Bi}}^* > 0.16$ . Under this condition, it was clear from the  $\text{H}_2$  TDS spectra that  $\text{C}_6\text{H}_6$  is not

the only hydrocarbon adsorbed on the surface. Experiments were performed in which 1.2 L of cyclohexene was dosed onto clean Pt(111) at  $\sim 100$  K. The surface was then flashed briefly to 350 K (presumably to produce benzene and the unidentified adsorbed intermediate(s) and to desorb cyclohexene and hydrogen) and finally postdosed with various Bi coverages between 0.2 and 1 at  $\sim 125$  K prior to TDS. In all these BPTDS experiments the *only* hydro-



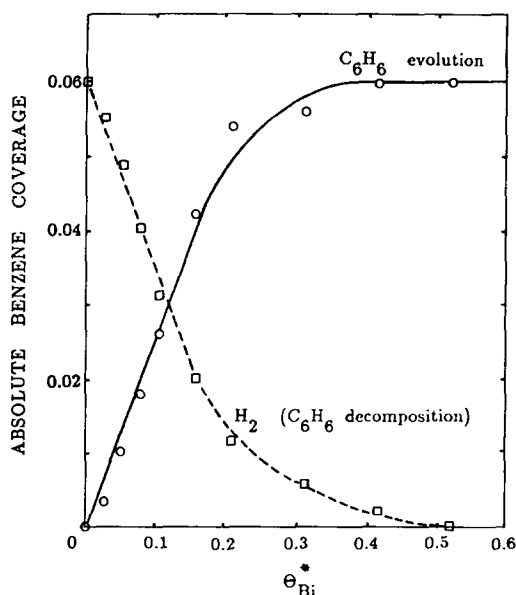


FIG. 12. Effect of Bi postdosing coverage upon the areas of the TDS peaks of Fig. 11 for  $H_2$  or decomposition ( $\square$ , dashed curve) and for molecular  $C_6H_6$  evolution ( $\circ$ , solid curve) from 0.28 L  $C_6H_{10}/Pt(111)$  which was preheated to 360 K. The peak areas were scaled to absolute benzene coverage units using a calibration based upon XPS results (see Section III.1.2).

carbon detected with the mass spectrometer as a desorption product was benzene. In particular, neither  $C_2H_2$ ,  $C_2H_4$ ,  $C_2H_6$ , nor cyclohexadiene was observable. Furthermore,  $H_2$  evolution was not completely suppressed, but only shifted to higher temperatures. This fact either rules out the presence of these species adsorbed in appreciable concentrations on the surface or suggests that the unidentified adsorbed intermediate(s) has (have) an activation energy for desorption greater than that of benzene, and they therefore dehydrogenate as benzene desorbs and creates free sites.

#### IV. DISCUSSION

Our results show that for high exposures ( $>1.5$  L) four different molecular  $C_6H_{10}$  desorption states appear in the thermal desorption spectra of cyclohexene on Pt(111) (see Section III.1.1). We have assigned the two highest temperature peaks to desorp-

tion of cyclohexene molecules di- $\sigma$ -bonded to the Pt surface through the carbons originally forming the double C-C bond (300 K) and agostically bonded to the Pt surface through the aliphatic hydrogens (255 K), respectively. The intermediate peak at 190 K was assigned to desorption of the second monolayer (and some minor edge effects), and the peak at lowest temperature (158 K) to multilayer desorption. Assuming first-order desorption and a typical preexponential factor of  $10^{13} s^{-1}$  for all the states, a standard, first-order Redhead analysis (18) yields desorption activation energies of 9.1, 11.0, 15.0 and 17.9 kcal/mole for the desorption peak temperatures of 158 K (multilayer), 190 K (second monolayer), 255 K (monolayer,  $\gamma$ -state), and 300 K (monolayer,  $\lambda$ -state), respectively. (For the multilayer peak, we used a coverage which gave a multilayer coverage of approximately one equivalent monolayer, so that this first-order treatment is fairly accurate for estimating the activation energy. This peak eventually becomes zero-order, with a constant leading edge.) Since adsorption occurs readily at  $\sim 100$  K and it is apparently non-activated, the activation energies for desorption listed above can be taken as estimates of the heats of adsorption on clean Pt(111). In the case of the multilayer peak, the value of 9.1 kcal/mole compares favorably with the heat of sublimation of pure cyclohexene ( $\sim 8.7$  kcal/mole (19)). The TDS results from cyclohexene on Bi/Pt(111) in Fig. 8 indicate a cyclohexene molecular desorption temperature of 170 K for one monolayer of Bi. Employing this temperature and the method mentioned above, we estimate an activation energy of 9.9 kcal/mole for cyclohexene desorption from Bi/Pt(111) ( $\Theta_{Bi}^* = 1.0$ ). This testifies to the weakness of the cyclohexene-Bi interaction, also noted in other studies (9-12) of hydrocarbons on Bi/Pt(111).

Our XPS results from heating a saturated monolayer of cyclohexene on clean Pt(111) to ever increasing temperatures (Figs. 5c-5e) suggested that the adlayer composition

was mostly of  $sp^3$ -type carbons at 222 K, was a mixture of  $sp^3$ - and  $sp^2$ -type carbons at 273 K, and was mostly  $sp^2$  carbon by 325 K. Our TDS results suggested that a mixture of both di- $\sigma$ -bonded ( $\lambda$ ) and agostically bonded ( $\gamma$ )  $C_6H_{10}$  should be on the surface at 222 K. All the carbon atoms should be  $sp^3$ -hybridized in di- $\sigma$ -bonded  $C_6H_{10}$  and two-thirds of them should be  $sp^3$ -hybridized in agostically bonded  $C_6H_{10}$ . The  $sp^3$ -like character of the C(1s) spectrum at 222 K suggests that the admixture contains a dominant amount of di- $\sigma$ -bonded  $C_6H_{10}$ . The XPS results further show that, by 273 K, a small amount ( $\sim 17\%$ ) of the  $C_6H_{10}$  has desorbed in the  $\gamma$ -TDS peak and substantial dehydrogenation of the remaining adsorbate has begun. By 325 K, desorption of cyclohexene and hydrogen adatoms is complete, and approximately 75% of the original monolayer remains on the surface. The stoichiometry of the adlayer at this point is approximately C : H = 6 : 7.5, which would be consistent with a 50 : 50 mixture of benzene and  $\pi$ -allyl c- $C_6H_9$ . In such a mixture, 75% of the carbon atoms would be  $sp^2$ -hybridized, which is consistent with the dominant  $sp^2$ -like position for the C(1s) peak. Similarly, when  $\Theta_{\text{H}_i}^{\text{H}_i} = 0.26$  (see Figs. 6–8), desorption of cyclohexene and hydrogen adatoms is complete by 350 K. At this point, the stoichiometry of the adlayer is approximately C : H = 6 : 8.4. This would be consistent with a 80 : 20 mixture of adsorbed c- $C_6H_9$  and benzene. A  $\pi$ -allyl species is attractive for the new intermediate here since it is consistent with both the C(1s) spectrum and the required stoichiometries, and it is often seen as the initial intermediate in dehydrogenation of olefins in late transition metal complexes (23).

The thermal desorption spectra from cyclohexene adsorption on Pt(111) have not been previously presented, except in very qualitative terms. Tsai *et al.* (3) claim that dehydrogenation of adsorbed cyclohexene to adsorbed benzene did not proceed at 298 K on Pt(111). This observation is not completely consistent with our results, which

suggest substantial dehydrogenation of adsorbed cyclohexene already by 273 K, and extensive dehydrogenation to produce a mixture of benzene and a new intermediate (perhaps  $\pi$ -allyl c- $C_6H_9$ ) by 325 K. However, the only probe for adsorbed benzene used by Tsai *et al.* was displacement by phosphine. In TDS after adsorbing benzene on clean Pt(111), there are two broad molecular desorption peaks, at 350 and 500 K (9). While the low-temperature state is likely to be displaceable with phosphine at 298 K, the low-coverage, higher-temperature state is probably not displaceable at this temperature. It is only this lower-coverage state of adsorbed benzene which is produced below 350 K from  $C_6H_{10}$  adsorption, as is evidenced by the benzene TDS of Fig. 3. Therefore, Tsai *et al.* (3) were unlikely to have seen this state by phosphine displacement. Results which suggest that  $C_6H_{10,a}$  should already convert to adsorbed benzene below 275 K at low coverages are reported observations of the reactions c- $C_6H_{12,a} \rightarrow$  c- $C_6H_{6,a} + 6H_a$  by 240 K on Pt(111) (10), and di- $\sigma$ -c- $C_5H_{8,a} \rightarrow$  c- $C_5H_{5,a} + 3H_a$  by 265 K on Pt(111) (8).

Tsai *et al.* (3) also report a peak at 403–413 K for benzene desorption from  $C_6H_{10}/$  Pt(111), and peaks for hydrogen evolution at 403, 443, 533, and 653 K. The positions of these peaks are in good agreement with those observed in our experiments for  $C_6H_{10}$  exposures larger than 1.5 L (see Section III.1).

During the cyclohexene TDS and BPTDS experiments on clean or Bi-dosed Pt(111), no cyclohexadiene was ever detected with the mass spectrometer as a desorption product from the surface. In a similar way, Gland *et al.* (4) observed no production of cyclohexadiene in their study of the low-pressure catalytic dehydrogenation of  $C_6H_{10}$  on Pt(111). These results suggest that, if adsorbed cyclohexadiene is produced as an intermediate during dehydrogenation, it is relatively unstable and accumulates only in very low concentrations on the surface. For  $C_6H_{10}$  adsorbed on

Ru(100), Flynn *et al.* (22) found evidence of extensive C–H and C–C bond breaking ( $H_2$  and ethylene main desorption products). No products of C–C bond breaking ( $C_2H_2$ ,  $C_2H_4$ , and  $C_2H_6$ ) were detected in our desorption experiments for  $C_6H_{10}$  adsorbed on Pt(111), which attests to the stronger tendency for C–C bond cleavage on Ru surfaces, compared to Pt surfaces.

Our results for small exposures of  $C_6H_{10}$  indicate that at low coverages (i.e., conditions in which there is a high number of free sites on the surface), the dehydrogenation of adsorbed cyclohexene to benzene occurs following a mechanism in which four C–H bonds are broken before  $\sim 350$  K. It is not obvious whether this mechanism involves simultaneous scission of the four C–H bonds in a concerted step or dehydrogenation through species of composition between  $C_6H_9$  and  $C_6H_7$  which further decomposes before 350 K. However, the concerted mechanism is unlikely on the basis of the extremely low preexponential factor expected. For large exposures of  $C_6H_{10}$  (i.e., conditions characterized by a very small number of free sites on the surface), the dehydrogenation of adsorbed cyclohexene to benzene follows a mechanism in which *not* all four C–H bonds are broken before 350 K. Instead, a new intermediate of stoichiometry between  $C_6H_9$  and  $C_6H_8$  is formed and stabilized at 350 K. This suggests that partial dehydrogenation of cyclohexene to this new intermediate requires fewer Pt sites (i.e., a smaller ensemble) than full dehydrogenation to adsorbed benzene. This new intermediate only further dehydrogenates at higher temperatures when benzene desorption creates new free Pt sites. The BPTDS experiments indicate that cyclohexadiene is not formed in appreciable amounts in the second mechanism and that the formed intermediate has an activation energy for desorption larger than that of adsorbed benzene. The  $\pi$ -allyl  $c$ - $C_6H_9$  species suggested above for this intermediate would have no direct gas-phase analog except as a very unstable radical or

ion, which would be consistent with its absence in TDS and BPTDS.

Our XPS results indicate that the saturation coverage of molecularly adsorbed cyclohexene on Pt(111) ( $\gamma$ - plus  $\lambda$ -states) is  $\sim 0.23$  molecule per Pt atom. This value indicates that above 4.5 Pt(111) surface atoms are required on *average* to accommodate each adsorbed cyclohexene molecule.

The decrease in the dehydrogenation probability of cyclohexene during TDS with increasing Bi precoverage (see Fig. 9) is similar to that reported for cyclopentene on Bi-covered Pt(111) (11). The dehydrogenation decays much less precipitously with  $\Theta_{Bi}^*$  for  $C_6H_{10}$  than for cyclohexane (10), cyclopentane (12), or benzene (9). In a previous publication (7) a kinetic model was developed to quantitatively treat the influence of  $Bi_a$  upon the competition between desorption and dehydrogenation in the surface reactions of cyclohexane, benzene, cyclopentane, and cyclopentene adsorbed on Pt(111). This model relies on the fact that Bi adatoms can be considered almost ideal site blockers, with very little electronic influence upon the coadsorbed hydrocarbon and its reactions. The central equation of the kinetic model is that the dissociation or dehydrogenation rate decreases with  $\Theta_{Bi}$  as

$$\text{rate} = k_{dt} (1 - n\Theta_{Bi})^A, \quad (1)$$

where  $n$  is the number of Pt atoms blocked by each Bi atom ( $\leq 3$ ) and  $A$  represents the number of additional vacant Pt sites that are simultaneously required for dissociation of an (already) adsorbed hydrocarbon molecule. Thus,  $A$  represents the ensemble size requirement to convert the adsorbed hydrocarbon into dehydrogenation products. No attempt has been made to obtain a quantitative kinetic fit with this model to the data in Fig. 9 because, for cyclohexene, Bi addition may cause a change in the pathway of dehydrogenation (see Section II.2.1), or at least a large change in the  $H_2$  TDS peak structure (see Fig. 6). Thus, for  $\Theta_{Bi}^* < 0.1$ , one reaction pathway dominates; but, for  $\Theta_{Bi}^* > 0.2$ , a second reaction path-

way takes control. This is probably because the latter reaction has a smaller "effective" ensemble requirement than the former. As noted above, this difference may simply be the fact that the latter reaction stops at a lesser degree of dehydrogenation ( $C_6H_{9,a}$  vs  $C_6H_{6,a}$ ) because there are no more free sites for hydrogen abstraction. Thus, an intermediate ( $C_6H_{9,a}$ ) which is relatively unstable on the clean surface (compared to adsorbed benzene +  $H_a$ ) may be kinetically stabilized due to the absence of free sites.

A detailed comparison of the data for dehydrogenation of cyclohexene on Pt(111) and the results for other cyclic hydrocarbons is presented in Ref. (7). A major feature of the data of Fig. 9 is the sigmoidal shape of the plot of  $p_{diss}$  versus  $\Theta_{Bi}^*$ , where it appears that some finite critical Bi coverage ( $\sim 0.3$ ) is required before any suppression in dissociation occurs. The reason for this sigmoidal behavior has been related (7) to the fact that the adsorbed cyclohexene can make several unsuccessful dissociation attempts as it migrates across the surface before it dehydrogenates or finally desorbs. In kinetic terms, this means that the rate constants for diffusion and dissociation of  $C_6H_{10}$  on clean Pt(111) are considerably larger than that for desorption. This is consistent with the results for other di- $\sigma$ -bonded alkenes on Pt(111) (7, 25) and with the ratio of rate constants for dehydrogenation:desorption of  $>50$  found from our present TDS results on clean Pt(111) in the limit of low coverage. Because of this large ratio, the probability for dehydrogenation of cyclohexene decays much more slowly with  $\Theta_{Bi}^*$  than, for example, that of benzene or cyclohexane (7). Thus, cyclohexene has a much smaller "effective ensemble requirement" for dehydrogenation (7).

#### ACKNOWLEDGMENTS

Acknowledgement is made to the Donors of the Petroleum Research Fund, administered by the American Chemical Society, for support of this research. Helpful discussions with Jeffrey Stryker and Malcolm Chisholm are a pleasure to acknowledge. Sincere ap-

preciation for typing of the manuscript is extended to Beth McGaw.

#### REFERENCES

1. Davis, S. M., and Somorjai, G. A., in "The Chemical Physics of Solid Surfaces and Heterogeneous Catalysis" (D. A. King and D. P. Woodruff, Eds.), Vol. 4, Chap. 7. Elsevier, Amsterdam, 1984.
2. Sinfelt, J. H., in "Catalysis, Science and Technology" (J. R. Anderson and M. Boudart, Eds.), Vol. 1, Chap. 5. Springer-Verlag, Berlin 1981.
3. Tsai, M. C., Friend, C. M., and Meutterties, E. L., *J. Amer. Chem. Soc.* **104**, 2539 (1982).
4. Gland, J. L., Baron, K., and Somorjai, G. A., *J. Catal.* **36**, 305 (1975).
5. Smith, C. E., Biberian, J. P., and Somorjai, G. A., *J. Catal.* **57**, 426 (1979).
6. Davis, S. M., and Somorjai, G., *Surf. Sci.* **91**, 73 (1980).
7. Campbell, C. T., Campbell, J. M., Dalton, P. J., Henn, F. C., Rodriguez, J. A., and Seimanides, S. G., *J. Phys. Chem.*, in press.
8. Campbell, C. T., Rodriguez, J. A., Henn, F. C., Campbell, J. M., Dalton, P. J., and Seimanides, S. G., *J. Chem. Phys.* **88**, 6585 (1988).
9. Campbell, J. M., Seimanides, S. G., and Campbell, C. T., *J. Phys. Chem.*, in press.
10. Rodriguez, J. A., and Campbell, C. T., *J. Phys. Chem.*, in press.
11. Henn, F. C., Dalton, P. J., and Campbell, C. T., *J. Phys. Chem.*, in press.
12. Campbell, J. M., and Campbell, C. T., *Surf. Sci.*, in press.
13. Summers, R. L., Nasa Technical Note TD-D-5285, National Aeronautics and Space Administration, Washington, DC, June 1969.
14. (a) Christmann, K., Ertl, G., and Pignet, T., *Surf. Sci.* **54**, 365 (1976); (b) Collins, D. M., and Spicer, W. E., *Surf. Sci.* **69**, 85 (1977).
15. (a) Steininger, H., Lehwald, S., and Ibach, H., *Surf. Sci.* **123**, 264 (1982); (b) Biberian, J. P., and Van Hove, M. A., *Surf. Sci.* **138**, 361 (1984).
16. Paffett, M. T., Campbell, C. T., and Taylor, T. N., *J. Chem. Phys.* **85**, 6176 (1986).
17. Wandelt, K., *J. Vac. Sci. Technol. A* **2**, 802 (1984).
18. Redhead, P. A., *Vacuum* **12**, 203 (1962).
19. The estimate value of 8.78 kcal/mole was obtained by adding the heats of fusion (0.787 kcal/mole, (20)) and vaporization (7.922 kcal/mole, (21)) of cyclohexene.
20. "Handbook of Chemistry and Physics" (R. C. Weast and M. J. Astle, Eds.), 61st ed., p. C-680. CRC Press, Boca Raton, 1980.
21. Letcher, T. M., and Marsicano, F., *J. Chem. Thermodynam.* **6**, 509 (1974).
22. Flynn, D. K., Polta, J. A., and Thiel, P. A., *Surf. Sci.* **185**, L497 (1987).

23. Collman, J. P., Hegedus, L. S., Norton, J. R., and Finke, R. G., "Principles and Applications of Organotransition Metal Chemistry," p. 179. University Science Books, Mill Valley, CA, 1987.
24. Paffett, M. T., Campbell, C. T., Windham, R. G., and Koel, B. E., *Surf. Sci.*, in press.
25. Windham, R. G., Koel, B. E., and Paffett, M. T., *Langmuir* **4**, 1113 (1988).
26. Wagner, C. D., Riggs, W. M., Davis, L. E., Moulder, J. F., and Muilenberg, G. E., "Handbook of X-Ray Photoelectron Spectroscopy." Perkin-Elmer, MN, 1978.